FIELD STUDY ON ONSHORE-OFFSHORE SEDIMENT TRANSPORT

by

Masataro Hattori*

ABSTRACT

The mechanism of onshore-offshore sediment transport and the process of beach profile evolution were studied through field investigations performed at Oarai Beach, Japan. The principal data set consists of twenty-four profile surveys taken at hourly intervals on each of two parallel lines spaced 10 m apart and of length 150 m. The lines extended from the backshore of the beach to a point on the sea bottom at a depth where no sand movement occurred. Simultaneous measurements of the waves and wave-induced currents were also made; the essential requirement of two-dimensionality was found to hold during the experiment. The profiles were used to calculate the net sediment transport rate on-offshore, and for an empirical eigenfunction analysis. A negative correlation was found between the transport direction (and resultant bottom change) and the mean sea level change. The sediment transport rate in the foreshore region was found to be proportional to the wave power, whereas outside the surf zone and near the breaker position it was proportional to the tractive force.

1. INTRODUCTION

Many laboratory studies have been undertaken to investigate the mechanism of onshore-offshore sediment transport on wave-formed beaches. However, there are several problems involved in transferring laboratory results to the prototype, such as the similarity law of movable bed models, scale effects, and so on. On real beaches, onshore-offshore sediment transport produced by waves and wave-induced currents occurs under very complicated conditions. It depends not only on the characteristics of the incident waves and bed material, but also on the specific location and bed form in the nearshore zone.

To understand the phenomena of sediment transport, more knowledge of the spatial and temporal dependence of the net rate and direction of transport is necessary. If adequate prototype data are available, onshore-offshore sediment transport as well as beach profile evolution can be inferred quantitatively with the aid of laboratory results. However, no analogous field studies have been performed because it is difficult to find sites where two-dimensionality in coastal processes is dominant. This paper reports such a field study made on onshore-offshore sediment transport processes.

---

* Professor, Department of Civil Engineering, Chuo University, Kasuga, Bunkyo-ku, Tokyo 112 JAPAN

The principal aims of this study are as follows:

(1) To relate the sediment transport rate to the onshore-offshore current velocity near the bottom.

(2) To clarify processes of sediment transport and beach profile evolution about the mean sea level due to the tide.

(3) To give a physical interpretation of the results by analysis of the beach profile.

Since this study aimed to investigate the onshore-offshore sediment transport in relation to beach profile change, it was necessary to measure accurately the bottom level changes along one or more lines running offshore. Many field studies have been made of the change in beach profile under waves in order to study the mechanism of sediment transport and the process of seasonal beach change. In only a few studies (e.g., Inman and Ruwnak, 1956; Nordstrom and Inman, 1975) were accurate measurements of the beach profile change performed. In most of the other studies, the profile data were usually contaminated by inaccuracies in the measurements. This resulted in difficulties in interpretating the phenomena of interest.

In laboratory experiments using two-dimensional wave flumes, the net rate and direction of the onshore-offshore sediment transport are usually calculated from a time series of bottom profile data by use of the continuity equation for bottom material (e.g., Watanabe, Riho and Horikawa 1982; Hattori and Kawamata 1982),

$$\frac{\partial h}{\partial t} = \frac{1}{(1-\lambda)} \frac{\partial q_x}{\partial x} \tag{1}$$

in which $h(x,t)$ is the water depth, q_x is the sediment transport rate on-offshore (along the x-axis), λ is the porosity of the bottom sediment, and t is the time. The coordinate system and notation are shown in Fig. 1.

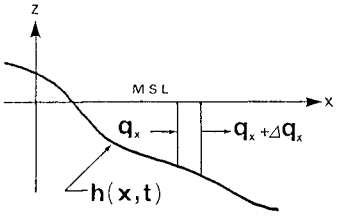

Fig. 1 Coordinate system and notation.

A preliminary experiment (Hattori and Komatsu, 1980) made in 1979 at the same study site (described below) indicated that the method of calculating the sediment transport rate in laboratory experiments could be applied to the field, if accurate measurements of the bottom change could be made. Based on this conclusion, a linear pole array technique was employed to measure the bottom level at fixed points on the beach.

2. EXPERIMENTAL PROCEDURE

2.1 Study Site

The field experiment was performed in August 1980 at Oarai Beach, Ibaragi Prefecture. The study area is a sandy beach with uncomplicated bathymetry, and is located adjacent to Oarai Harbor facing the Pacific Ocean (Fig. 2). The local beach material is quartz sand of median diameter 0.18 mm. Nearshore bottom profiles were measured by means of two linear pole arrays (labelled A and B in Fig. 2). The site selected for placement of the pole arrays was located 200 m north of the jetty. Diffraction at the breakwater 1400 m seaward produces relatively calm wave conditions of exceptional two-dimensionality. The pole arrays were of sufficient length to extend beyond the critical depth of sand movement during the experiment.

The spacing between the poles was 2 m and the total length of the pole arrays was 150 m. A reference point was defined, located on the backshore and landward of the maximum runup of swash. The pole array consisted of steel pipes 6.4 cm in diameter and 2 m to 5 m long. The pipes were driven into the sand bottom to a depth of about 1 m by means of a jet water pump.

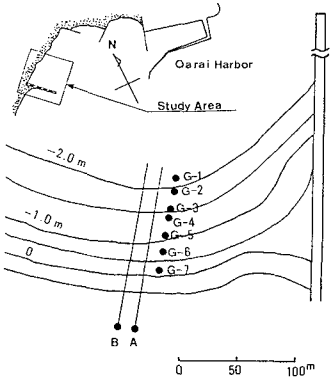

Fig. 2 Map of the study site.

Simultaneous measurements of the waves and wave-induced currents were made with capacitance-type wave gages and two-component electromagnetic current meters at seven locations indicated by G-1 to G-7 in Fig. 2. The seven wave gage stations were alined 10 m east of pole array A.

2.2 Profile survey

Surveys along the pole arrays were made every hour to yield a time series of the profile data over the 24-hr experiment period. Positions of the poles and absolute elevations of the pole tops were measured by using standard survey techniques and a bench mark on the backshore, which was derived from a permanent bench mark. Two supplemental reference points for measuring bottom level elevation were marked on each pole at distances of 1 m and 2 m. The height of the reference point from the bottom was measured by reading the scale of a survey rod, specially designed to avoid scouring around the pole and rod. From the survey result for the elevation of the tops of the poles, the bottom depth could be determined. The estimated accuracy of the absolute elevation of the bottom level was about 0.5 cm. The beach profile surveys were completed within about 15 min.

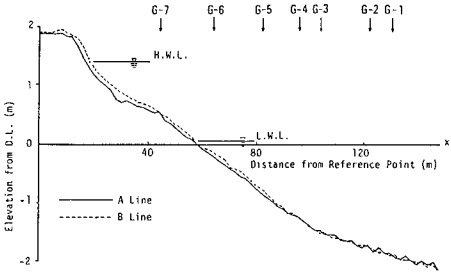

Fig. 3 Mean beach profiles at the study site.

Figure 3 illustrates mean beach profiles along the pole arrays, which were obtained by averaging the 24 sets of profile data taken over the experimental period. Arrows at the top of the figure indicate the positions of wave gage stations, G-1 to G-7. Figure 4 shows the positioning survey results of the pole arrays and wave gage stations. Pole positions are indicated by solid and open circles. The two pole arrays formed almost straight lines.

2.3 Instrumentation

Simultaneous measurements of the waves and wave-induced currents on the study beach are essential to understand the processes of sediment transport, and to confirm two-dimensionality of the various phenomena. Each wave gage station consisted of a capacitance-type wave gage and a two-component electromagnetic current meter. The wave gage, developed by Sato et al. (1980), has a superior frequency response than other conventional field wave gages, but has the shortcoming that the output signal level sometimes is reduced due to adherence of polluted sea water film to the capacitance line.

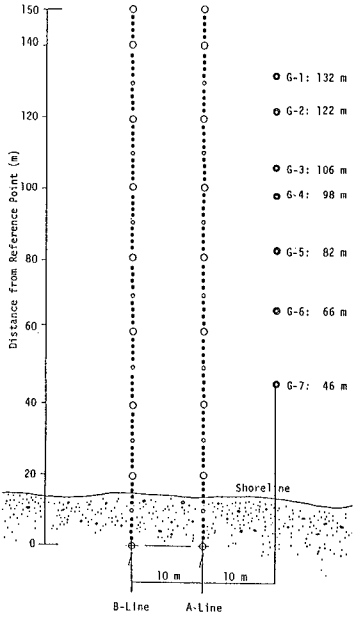

Fig. 4 Positioning survey results of the pole arrays and wave gage stations.

The current meters, used for measurements of the wave-induced current velocity, were fixed to steel frames at a height of 20 cm from the bottom of the frame. They were set on the sea bottom so that one of the two transducer axes was directed on-offshore. To supplement the measurements of the local wave characteristics on the beach, additional wave measurements were made about 200 m seaward of the tip to the jetty by means of a linear array of three pressure sensors (Fig. 5).

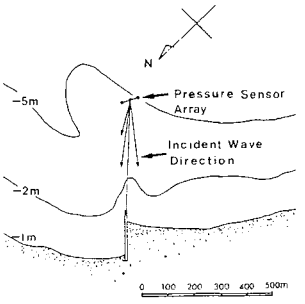

Fig. 5 Location of the pressure sensor array and the directional distribution of incident waves.

2.4 Data analysis

The survey data of the bottom level for each pole array were punched on cards for computer input and then stored on a magnetic disk for plotting profiles and for calculating the transport rate of sediment transport. Output of the wave gages and electromagnetic current meters was recorded on open-reel digital data recorders with a sampling interval of 0.2 s. Statistical characteristics of the waves and current velocities were calculated for each 16 min. of the collected data. In these calculations, wave components longer than 25 s entering in the free surface and in current velocity variations were cut off by using a high pass filter. The mean sea level variation on the study beach was not measured. Instead, the tide gage record at Oarai Harbor was used.

3. WAVE AND CURRENT VELOCITY

3.1 Characteristics of incident waves in the offshore

Figure 6 shows time histories of significant wave height and period measured at the pressure sensor array (Fig. 5), and the tide gage record at Oarai Harbor. This figure indicates that wave height and period in the offshore zone were almost constant over the duration of the experiment, 0.35 m and 7.3 s, respectively. The distribution of the incident wave direction obtained at the pressure sensor array is also given in Fig. 5. It is noticed from this figure that waves were incident normal to the study beach.

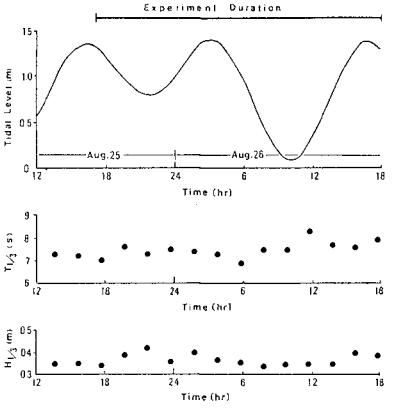

Fig. 6 Time histories of incident wave height and period at the pressure sensor array (Fig. 5) and tide gage record at Oarai Harbor.

Figure 7 gives examples of the record monitors of the free surface variations, η , at wave gage stations G-3 to G-7. It is seen that the waves proceeded to Station G-5 without wave breaking and that the breaking position was located near Station G-6. Solid lines on this figure indicate the propagation process of the marked wave.

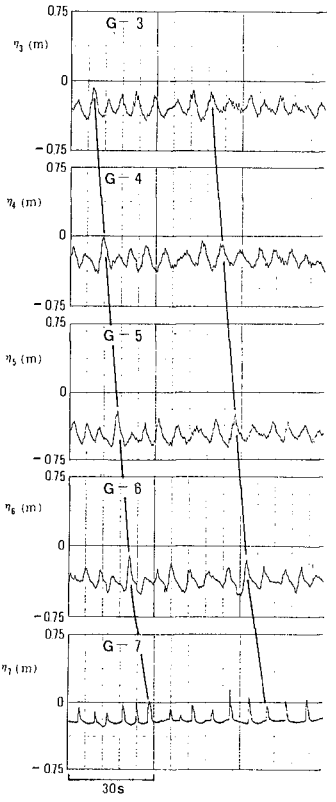

Fig. 7 Comparisons of the records of the free surface variation at Stations G-3 to G-7.
G-3 to 5: outside the surf zone,
G-6: near the breaker position,
G-7: inside the surf zone.

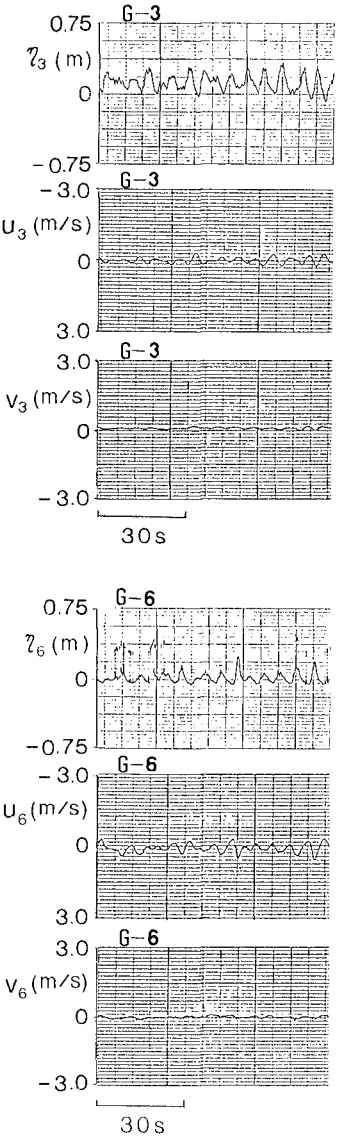

Fig. 8 Comparison of records of the free surface variation and of the on-offshore and longshore current velocities at Stations G-3 and G-6.

Figure 8 gives comparisons of monitor records of the free surface variation and of the on-offshore and longshore components of current velocity, U and V, respectively, at the wave gage stations G-3 and G-6. This figure clearly shows that the on-offshore current velocity fluctuated in phase with the free surface variation, and that the longshore component was very weak. Similar tendencies were observed at various locations on the beach over the entire duration of the experiment.

Based on the measured wave direction and current velocity, it is concluded that the coastal processes of interest on the beach maintained two-dimensionality, an essential requirement for this study.

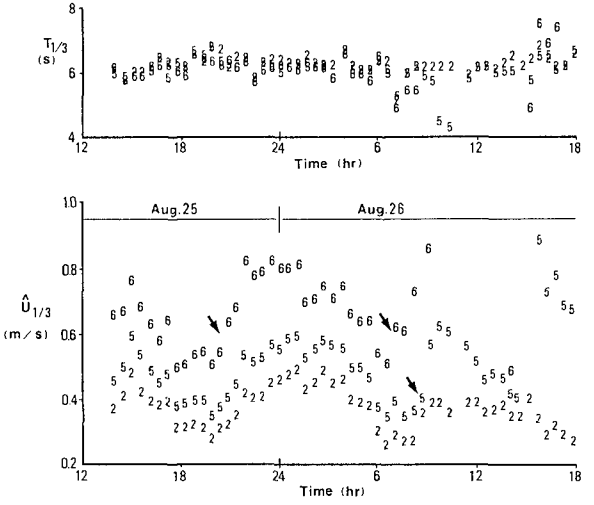

Fig. 9 Time histories of $\hat{U}_{1/3}$ and $T_{1/3}$ of the on-offshore current velocity at Stations G-2, G-5, and G-6.

Figure 9 illustrates time histories of the significant full amplitude and period of the on-offshore current velocity, $U_{1/3}$ and $T_{1/3}$. Plotted numbers represent the wave gage station where the data were taken. The velocity amplitude varies with the variation of the mean sea level due to the tide, but the period is almost constant (about 6.3 s).

According to Fig. 5, the mean period of the incident waves at the pressure sensor array is about 7.3 s, which is longer than the period derived from the on-offshore current velocity. Two factors may be pointed out as reasons why this difference in measured period occurred: (1) The frequency response of the electromagnetic current meter, 10 Hz, is higher than that of the pressure sensor. (2) In analysis of the on-offshore current velocity, the long period components were removed by a high-pass filter. The mean period of the incident waves was therefore taken to be 6.3 s for the experiment period.

Interesting behavior of the time histories of $\hat{U}_{1/3}$ can be noted. Rapid increase of $U_{1/3}$, indicated by thick arrows, indicates that the breaker position, in a statistical sense, was located near or at the wave gage station where the current velocity data were taken.

Since the longshore component of the current velocity was very weak, its mean with respect to time was negligibly small. On the other hand, a steady component of the on-offshore current velocity, $\bar{U}$, was observed at various locations of the beach. Figure 10 illustrates time histories of $\bar{U}$ at the wave gage stations G-2, 5, and 6. From this figure, it was found that, except during the rising period of sea level, from 14 hr to 17 hr Aug. 26, the steady current velocity was much lower than the maximum water particle velocity due to wave motion and was directed offshoreward. It is considered that this current did not have any significant influence on the onshore-offshore sediment transport.

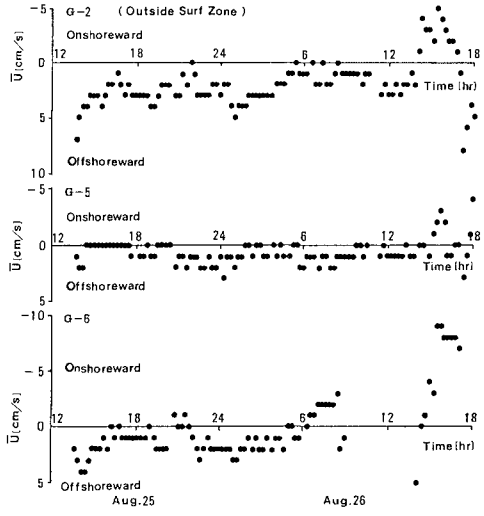

Fig. 10 Time histories of the steady on-offshore current velocity.

The breaking waves were mainly of the plunging type. The position of wave breaking was estimated by 1) visual observation facilitated by the pole arrays, 2) comparisons between time histories of the variations of the free surface and on-offshore current velocity (Huntley and Bowen, 1975), 3) rapid increase of the significant full amplitude of on-offshore current velocity (Fig. 9), and 4) spatial variation of the statistical characteristics of the waves and wave-induced currents.

4. RESULTS AND DISCUSSION ON THE SEDIMENT TRANSPORT

4.1 Net transport rate

The net rate of onshore-offshore sediment transport, q_x, was calculated from the time series of the profile measurements taken every two hours. Figure 11 shows the on-offshore distributions of q_x. In these calculations, the profile used was that given by the mean obtained from the two arrays. The numerals in the figure give the month, day, and time when the profile measurements were made. Locations of wave gage stations are indicated by arrows.

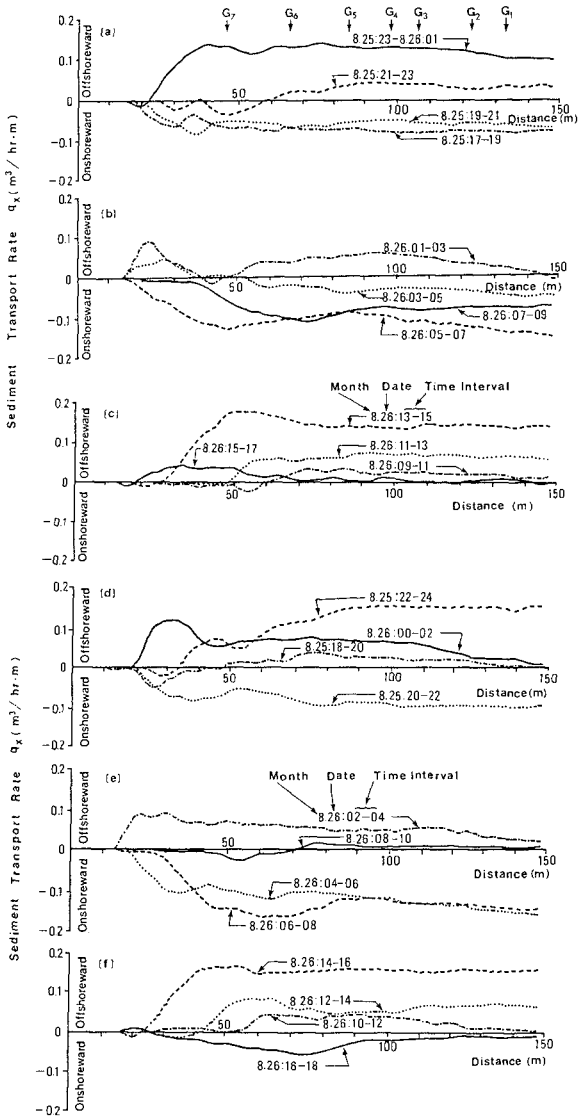

Fig. 11 Calculated results of the net rate of sediment transport.

It was found from the distributions of q_x that about half of the results did not satisfy the condition for the sediment budget. The distributions were calculated with the boundary condition $q_x = 0$ at the reference point on the backshore. Under calm sea conditions, sediment movement due to waves in the offshore zone is not active and bottom level changes are very small. When the change in sand level fell below 0.5 cm, inaccuracy in the profile measurements in the offshore led to a cumulative error in the calculation of q_x.

It was originally intended to express $|q_x|$ in terms of the significant full amplitude of the on-offshore current velocity, $\hat{U}_{1/3}$; however, no meaningful correlation could be found. This suggests the interesting possibility that sediment transport under irregular waves is mainly determined by the statistically averaged curreent velocity. It is therefore believed that the beach profile does not respond quickly to variations in current velocity caused by different incident wave forms. Instead of U_{max}, the maximum velocity of the on-offshore current velocity, for convenience the mean velocity $\hat{U}_{1/2}$ was used.

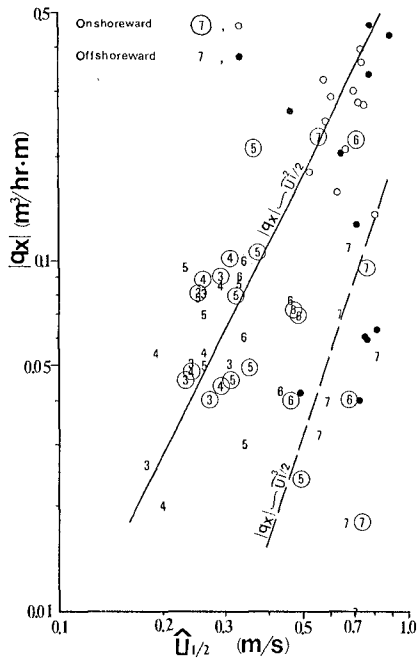

Fig. 12 Relationship between $|q_x|$ and $\hat{U}_{1/2}$.

The calculated absolute values of the net transport rates, $|q_x|$, at various locations were plotted against the mean full amplitude of the onshore-offshore current velocity, $\hat{U}_{1/2}$ as shown in Fig. 12. Numbers in the figure indicate the wave gage station. Filled and open circles denote data obtained in the preliminary experiment of 1979. Open circles and numbers in circles denote onshore transport, and filled circles and numbers without circles denote offshore transport.

Two distinct relationships between $|q_x|$ and $\hat{U}_{1/2}$ are apparent in Fig. 12. The solid line passes through the data obtained outside the surf zone and near the wave breaking position. The dashed line passes through the data obtained inside the surf zone. The slopes of the fitted lines are approximately 2.0 and 3.0 respectively. The standard expression for the shear stress acting on the bottom, τ_b, is given by

$$\tau_b = \frac{1}{2} \rho f_w u_{max}^2 \tag{2}$$

in which f_w is the wave friction coefficient, u_{max} is the maximum velocity near the bottom, and ρ is the density of the fluid. Although waves exhibit nonlinearities both inside and outside the surf zone, u_{max} will be replaced by $\hat{U}_{1/2}$. Thus Eq. (2) can be rewritten as

$$\tau_b = k \rho f_w \hat{U}_{1/2}^2 \tag{3}$$

where k is a coefficient representing the nonlinearity of the wave motion. Using Eq. (3), the two relationships in Fig. 12 can be written

$$|q_x| \sim \hat{U}_{1/2}^2 \sim \tau_b \qquad \text{(outside the surf zone and near breaking position)} \tag{4}$$

and

$$|q_x| \sim \hat{U}_{1/2}^3 \sim \tau_b \hat{U}_{1/2} \qquad \text{(inside the surf zone)} \tag{5}$$

The two empirically-based relationships between q_x and $\hat{U}_{1/2}$ expressed by Eqs. (4) and (5) indicate that two different processes of onshore-offshore transport can exist in the nearshore zone. In the present study, outside the surf zone and near the breaker position, the net transport rate was proportional to the tractive force acting on the bottom surface. Therefore, the dominant process of sediment transport was that of bed load. On the other hand, inside the surf zone, the net transport rate was proportional to the wave power, so that the dominant process was that of suspended load.

As seen in Fig. 11, the net transport rate varies with the distance offshore as measured from the reference point on the backshore. Figure 13 gives the time histories of the breaker position and location where the net transport rate takes a maximum value. From this figure, it can be noted that the maximum transport rate occurs near the breaker position.

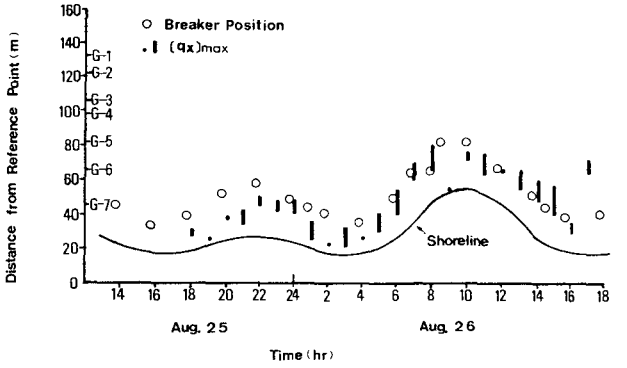

Fig. 13 Time histories of breaker position and location of $q_{x,max}$.

4.2 Direction of the Sediment Transport

To investigate effects of the mean sea level change due to the tide, temporal changes in the distributions of q_x were drawn schematically in Fig. 14, which gives the tidal record at Oarai Harbor. This figure clearly indicates that during ebb tide q_x was directed predominantly onshore, while during flood tide it was directed offshore. This suggests that the predominant direction of the net sediment transport on-offshore was governed significantly by the tide.

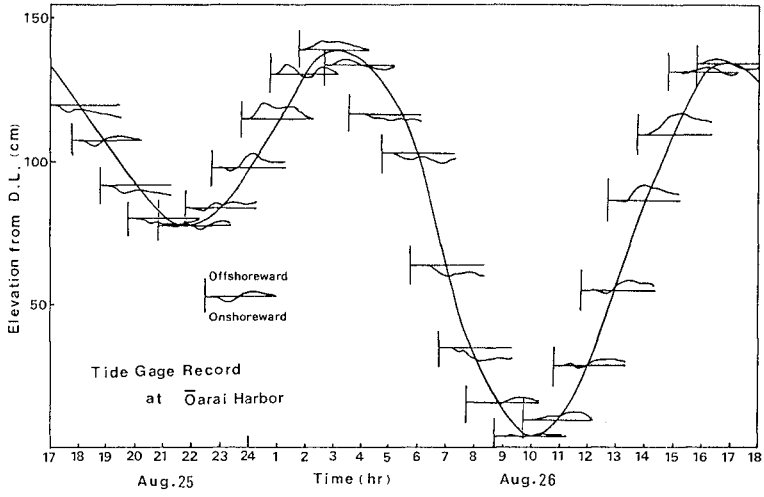

Fig. 14 Tide gage record and q_x distribution (Fig. 11).

As seen in Fig. 13, the range of the wave breaking position over the duration of the experiment covered a distance between 25 m to 80 m from the reference point. As the tide rose, the location of wave breaking advanced shoreward and the width of the surf zone became narrower, whereas when the tide fell, the surf zone became wider. From the mean beach profile in Fig. 3, the mean beach slope inside the surf zone during the high water period is estimated to be 1/20, and that during the low water period 1/32. Due to the beach cut pattern, the morphodynamic state of the surf zone and beach over a tidal cycle appeared to change from a reflective mode during the flood tide to a dissipative one during the ebb tide (Wright, 1982).

Hattori and Kawamata (1982) proposed a criteria for predicting the predominant direction of sediment transport on-offshore,

$$\frac{(H_o/L_o)\tan\beta}{(w_s/gT)} = C \begin{cases} > \\ 0.5 \\ < \end{cases} \begin{matrix} \text{(offshore transport)} \\ \\ \text{(onshore transport)} \end{matrix} \qquad (6)$$

in which H_o/L_o is the deepwater wave steepness, w_s is the fall velocity of the sediment, T is the incident wave period, $\tan\beta$ is the mean beach slope inside the surf zone, and g is the acceleration of gravity. The value of C during the high and low water periods are 0.76 and 0.47 respectively (H_o = 0.35 m, T = 6.3 s, d_{50} = 0.18 mm, and w_s = 2.3 cm/s). It is thus concluded from Eq. (6) that the direction of sediment transport during the flood tide was offshoreward whereas during the ebb tide it was onshoreward.

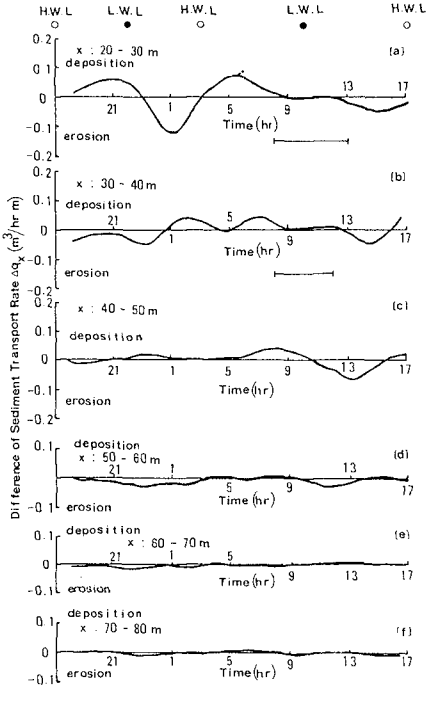

Fig. 15 Time histories of the rate of beach profile change inside the surf zone.

Figure 15 shows time histories of the difference of net transport rate, Δq_x, between adjacent locations inside the surf zone. This figure was obtained by using the q_x distribution curves given in Fig. 11. Horizontal solid lines indicate the duration the bed was dry during the ebb tide. At the top of the figure, the times of occurrence of H. W. L. and L. W. L. are indicated by open and filled circles. Since Δq_x expresses the rate of bottom change, comparison of these time histories indicates the trend of the beach profile evolution. During the flood tide, erosion on the upper beach was accompanied by sand accretion near the breaker position. During the ebb tide sand removed immediately from outside the surf zone was deposited on the low water terrace and foreshore. These trends of beach evolution support the hypothesis that the direction of net sediment transport is closely related to the change in the morphodynamic state of the beach over a tidal cycle.

5. DATA ANALYSIS BY EMPIRICAL EIGENFUNCTIONS

Seasonal patterns of onshore-offshore sediment movement and seasonal beach changes can be well described by means of the empirical eigenfunction technique. The application of this statistical technique promises to give further progress in our understanding of the process of beach profile evolution (Winant, Inman, and Nordstrom, 1975; Aubrey, 1979). The empirical eigenfunction technique was employed to analyze the profile data in order to get a more definite physical interpretation of the experimental results (Hashimoto and Uda, 1979).

The analysis was made taking into account the mean sea level due to the tide for the time series data of deviations from the arithmetic mean profile, as shown in Fig. 3 (Katoh, Tanaka, and Nadaoka, 1981). Since, in general, the data sets involve physical quantities with different units, each quantity was normalized so that its mean value was zero and its variance unity. The normalizing procedure is given in Eqs. (7) to (9).

$$F_{i,t} = (F_{i,t} - \bar{F}_i)/S \tag{7}$$

$F_{1,t} \sim F_{75,t}$: Bottom elevation

$F_{76,t}$: Sea level

$$\bar{F}_i = \frac{1}{n_t} \sum_{t=1}^{n_t} F_{i,t} \quad (n_t = 24) \tag{8}$$

$$S = \frac{1}{n_t - 1} \sum_{t=1}^{n_t} (F_{i,t} - \bar{F}_i)^2 \tag{9}$$

In these equations, $F_{i,t}$ is the physical quantity, (elevations of the bottom, and the sea level), $F'_{i,t}$ is the deviation of $F_{i,t}$ from the mean, $\bar{F}_i$ and S are the mean and variance of $F_{i,t}$. The subscript i is an index ranging between 1 and 76. The range from 1 to 75 covers the total number of points along the profile and the index 76 denotes the sea level. The subscript t is an index ranging between 1 and n_t, the total number of times the measurements were made (24).

The set of deviations from the mean value at time t, Φ_t, is given by Eq. (10),

$$\Phi_t = (F'_{1,t}, F'_{2,t}, \cdots\cdots, F'_{76,t})^T \tag{10}$$

where the superscript T is the matrix transpose operator. Then, Φ_t is expressed in terms of spatial and temporal eigenfunctions, e^*_n and $c^*_{n,t}$,

$$\Phi_t = \sum_{n=1}^{n_t} c^*_{n,t}\, e^*_n \tag{11}$$

where the subscript n denotes the order of the eigenfunction. Equation (11) means that the temporal characteristics of Φ_t is expressed by $c^*_{n,t}$. The correlation coefficient, $R_{n,i}$, between $c^*_{n,t}$ and $F^*_{i,t}$ is given by Eq. (12),

$$R_{n,i} = \sqrt{\lambda_n}\, e^*_{n,i} \tag{12}$$

in which λ_n is the n-th eigenvalue.

Since the index i indicates the location of the i-th pole from the reference point of the pole array, the relation between $R_{n,i}$ and i can be easily converted into a spatial dependence of R_n, which is equivalent to the spatial dependence of the eigenfunction e^*_n as shown by Fig. 16. The solid and broken lines in Fig. 16 represent the first and second eigenfunctions, respectively. The horizontal line at the top of the figure indicates the range of the breaking position.

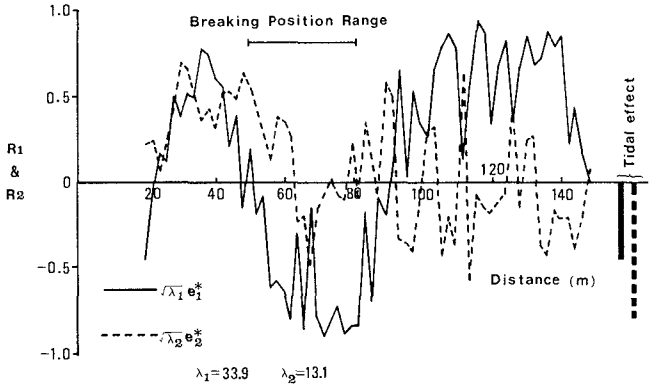

Fig. 16 Spatial dependence of the eigenfunctions, e^*_1 and e^*_2.

The first eigenfunction, e^*_1, exhibits a maximum near the foreshore, a broad maximum in the offshore, and a broad minimum over the range of the breaker position. In addition, e^*_1 indicates that a negative correlation exists between the effect of the tide and profile changes both in the foreshore and offshore, while a positive correlation exists over the range of breaker position. These results mean that as the tide fell, sand removed from the wave breaking zone was transported both shoreward and seaward, and was deposited on the foreshore and offshore.

The second eigenfunction, e_2^*, shows a broad maximum on the foreshore, but it does not exhibit any distinct dependence in the offshore. Since the correlation between the profile change and the tidal effect for e_2^* is stronger than that for e_1^*, e_2^* appears to represent the accretion of the foreshore caused by onshore sediment transport inside the surf zone due to seaward dislocation of the breaker position during the ebb tide. These interpretations of the spatial structures of e_1^* and e_2^* are supported by the time histories of beach profile change which are given in Fig. 15.

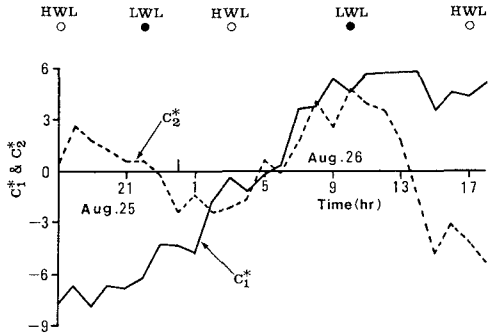

Fig. 17 Temporal dependence of the eigenfunctions c_1^* and c_2^*.

Figure 17 shows temporal variations of the eigenfunctions, c_1^* and c_2^*, denoted by solid and broken lines respectively. At the top of the figure, the times of occurence of H.W.L. and L.W.L. are indicated by open and filled circles. c_1^* shows a trend of gradual increase with time. This means that the study beach was accretive over the duration of the experiment (24 hr). On the other hand, the time dependence of c_2^* exhibits a strong periodicity indentical to that of the tide. During the ebb tide, the beach profile shows a tendency to accrete, while during the flood tide it shows an erosive tendency. Based on these temporal trends, the second temporal eigenfunction appears to adequately represent the profile change in the foreshore. It is thus substantiated by empirical eigenfunction anaysis that beach profile evolution as well as onshore-offshore sediment transport over a tidal cycle are greatly influenced by the mean sea level change caused by the tide.

6. CONCLUSIONS

The main conclusions from the present field study are now summarized.

(1) Two distinct relationships for the onshore-offshore sediment transport rate were found in the present experiment; i) the net transport rate was proportional to the tractive force acting on the bottom outside the surf zone and near the breaker position, and ii)

inside the surf zone the net rate was proportional to the wave power. The maximum transport rate occurred near the breaker position.

(2) The predominant direction of sediment transport during the flood tide was offshoreward, while during the ebb tide it was onshoreward. The effect of the tide on the direction of sediment transport was produced by the change in the morphodynamic state of the beach, as being either reflective or dissipative. The migration of the breaker position plays an important role in the change of beach characteristics.

(4) Analysis by the empirical eigenfunction method also indicated a negative correlation between the beach profile changes in the foreshore and offshore zones and tidal variation, while a positive correlation existed between the profile change and tide in the area of the breaker position.

(5) The first and second temporal eigenfunctions, respectively, were found to describe the evolutionary trend of the study beach and the trend of profile change in the foreshore, and were found to have the same periodicity as that of the tide.

ACKNOWLEDGEMENTS

The field work in this study was carried out through the sincere cooperation of many people, and I would like to thank all of them. In particular, I would like to express my appreciation to Mr. S. Hotta, Tokyo Metropolitan University, who suggested the idea of measuring beach profiles by means of a linear pole array system. I would also like to thank Dr. N. C. Kraus of the Nearshore Environment Research Center for proofreading the manuscript.

REFERENCES

Aubrey, D.G. (1979): Seasonal patterns of onshore/offshore sediment movement, J. Geophys. Res., Vol. 84, No. C10, pp. 6347-6354.

Hashimoto, H. and T. Uda (1979): Analysis of beach profile changes at Ajigaura by empirical eigenfunction, Coastal Eng. in Japan, JSCE, Vol. 22, pp. 47-57.

Hattori, M. and R. Kawamata (1982): Onshore-offshore transport and beach profile change, Proc. 17th Conf. on Coastal Eng. ASCE, pp. 1175-1194.

Hattori, M. and N. Komatsu (1980): Field experiments on on-offshore sediment transport and beach profile changes, Proc. 27th Japanese Conf. on Coastal Eng., JSCE, pp. 187-191. (in Japanese)

Huntley, D.A. and A.J. Bowen (1975): Comparison of the hydrodynamics of steep and shallow beaches, Chapter 4, Nearshore Sediment Dynamics and Sedimentation, Ed. by J. Hails and A. Carr, John Wiley & Sons, pp. 69-109.

Inman, D.L. and G.A. Ruwnak (1956): Changes in sand on the beach and shelf at La Jolla, California, B.E.B. TM-82, 30 pp.

Katoh, K., N. Tanaka, and K. Nadaoka (1981): Effects of tidal level and waves on two-dimensional deformation of foreshore, Proc. 28th Japanese Conf. on Coastal Eng., JSCE, pp. 207-211. (in Japanese)

Nordstrom, C.E. and D.L. Inman (1975): Sand level changes on Torrey Pines Beach, California, CERC, MP11-75.

Sato, M., K. Nakamura, and T. Tamura (1980): Field measurements of surf waves, Proc. 27th Japanese Conf. on Costal Eng., JSCE, pp. 124-128. (in Japanese)

Watanabe, A., Y. Riho, and K. Horikawa (1982): Beach profiles and on-offshore sediment transport, Proc. 17th Conf. on Coastal Eng., ASCE, pp. 1106-1121.

Winant, C.D., D.L. Inman, and C.E. Nordstrom (1975): Description of seasonal changes using empirical eigenfunctions, J. Geophys. Res., Vol. 80, No. 15, pp. 1979-1986.